

# Spherical Triboelectric Nanogenerators Based on Spring-Assisted Multilayered Structure for Efficient Water Wave Energy Harvesting

Tian Xiao Xiao, Xi Liang, Tao Jiang, Liang Xu, Jia Jia Shao, Jin Hui Nie, Yu Bai, Wei Zhong, and Zhong Lin Wang\*


Making use of water wave energy at large is one of the most attractive, low-carbon, and renewable ways to generate electric power. The emergence of triboelectric nanogenerator (TENG) provides a new approach for effectively harvesting such low-frequency, irregular, and “random” energy. In this work, a TENG array consisting of spherical TENG units based on spring-assisted multilayered structure is devised to scavenge water wave energy. The introduction of spring structure enhances the output performance of the spherical TENG by transforming low-frequency water wave motions into high-frequency vibrations, while the multilayered structure increases the space utilization, leading to a higher output of a spherical unit. Owing to its unique structure, the output current of one spherical TENG unit could reach 120  $\mu\text{A}$ , which is two orders of magnitude larger than that of previous rolling spherical TENG, and a maximum output power up to 7.96 mW is realized as triggered by the water waves. The TENG array fabricated by integrating four units is demonstrated to successfully drive dozens of light-emitting diodes and power an electronic thermometer. This study provides a new type of TENG device with improved performance toward large-scale blue energy harvesting from the water waves.

## 1. Introduction

Due to its central role in human life, energy has attracted worldwide attention in the past decades. Since the fossil fuels

T. X. Xiao, X. Liang, Dr. T. Jiang, Dr. L. Xu, J. J. Shao, J. H. Nie, Y. Bai, W. Zhong, Prof. Z. L. Wang  
CAS Center for Excellence in Nanoscience  
Beijing Key Laboratory of Micro-nano Energy and Sensor  
Beijing Institute of Nanoenergy and Nanosystems  
Chinese Academy of Sciences  
Beijing 100083, China  
E-mail: zlwang@gatech.edu

T. X. Xiao, X. Liang, Dr. T. Jiang, Dr. L. Xu, J. J. Shao, J. H. Nie, Y. Bai, W. Zhong, Prof. Z. L. Wang  
School of Nanoscience and Technology  
University of Chinese Academy of Sciences  
Beijing 100049, China  
Prof. Z. L. Wang  
School of Materials Science and Engineering  
Georgia Institute of Technology  
Atlanta, GA 30332-0245, USA

 The ORCID identification number(s) for the author(s) of this article can be found under <https://doi.org/10.1002/adfm.201802634>.

DOI: 10.1002/adfm.201802634

are finite resources, searching for other kinds of alternative energy sources is highly desirable.<sup>[1,2]</sup> Water wave energy is a promising energy source for large-scale applications due to both the abundant reserves and little dependence on environmental conditions.<sup>[3–6]</sup> Through decades of exploration, increased efforts have been devoted to harvesting such energy. However, most demonstrated generators are based on the electromagnetic induction effect, and they are usually cumbersome, complicated, and particularly inefficient at ocean wave frequencies.<sup>[7,8]</sup> Therefore, a new type of generator for water wave energy harvesting is a pressing need.

Triboelectric nanogenerator (TENG) based on the coupling effect of triboelectrification and electrostatic induction has emerged as a powerful technology for converting ambient mechanical energy into electric energy.<sup>[9–17]</sup> Different from conventional electromagnetic generators, TENGs originating from the Maxwell's

displacement current are based on the varying polarization field induced by surface polarization charges rather than the varying magnetic field to generate electricity.<sup>[18]</sup> Since its birth, different TENGs have been designed and utilized to harvest low frequency energies, such as energies from human motion, wind, and water waves.<sup>[19–31]</sup> Moreover, rolling spherical TENGs and coupled TENG networks have been demonstrated to harness the water wave energy, because of the advantages of lightweight, small-resistance under the water wave motions, and easy to be integrated, etc.<sup>[23,24,32]</sup> Nevertheless, the previous fabricated spherical TENGs for harvesting water wave energy have a low output current, which limits their practical applications. One possible solution is to change the working mode of TENG combined by introducing a spring structure into the sphere, which can store the kinetic energy from water impact and later convert into electric power via residual vibrations. Our previous works showed the spring-assisted structure can improve the output performance and efficiency of TENGs in water wave energy harvesting.<sup>[19,33]</sup>

Herein, combining the advantages of spring structure and integrated multilayered structure, we demonstrated a kind of spherical TENG with spring-assisted multilayered structure for harvesting water wave energy. The TENG works in

a contact-separation mode based on the triboelectricity between the aluminum electrode and polarized fluorinated ethylene propylene (FEP) film, which can produce higher current than spherical TENGs in single-electrode or freestanding mode. First, the output performance of the spherical TENG was measured in water as triggered by water waves. The effects of the frequency and amplitude of the water waves controlled by a function generator were investigated. Then the spherical TENG unit was optimized by adjusting both the basic unit number of the TENGs in the multilayered structure and the mass of copper block. Finally, a TENG array consisting of four optimized spherical units connected in parallel was fabricated and measured under the water waves. Triggered by the water waves, the TENG array produces an output current of 225  $\mu\text{A}$  and a maximum output power of 15.97 mW, which is a giant leap toward the blue energy dream compared with previous studies.

## 2. Results and Discussion

The structure of spherical TENG designed with spring-assisted multilayered structure floating on water surface is schematically shown in **Figure 1a**. The diameter of the outside shell is 10 cm, and four steel shafts are fixed by bottom and top circular acrylic blocks adhered on the internal wall of the sphere. Four flexible springs adhered on bottom acrylic block sustain the mass block, which consists of a copper block sandwiched in between two 2 mm thick circular acrylic blocks. Four rigid springs are attached on the top side of the mass part in order to protect the mass block from collision with top acrylic block and make use of the resilience force to press the multilayered TENGs under

fierce triggering of the water waves. The mass block and the springs move along the steel shafts. In addition, there are two 4 mm thick acrylic blocks attached on the bottom side of multilayered TENGs and bottom circular acrylic block to ensure a sufficient contact. And a 50  $\mu\text{m}$  thick Kapton film, which is shaped to a zigzag structure by making deformations at evenly spaced intervals, serves as the substrate for TENG units on both sides. The structure of the zigzag multilayered TENG is schematically shown from the enlarged view in **Figure 1a**. As sketched, the multilayered TENG consists of five TENG units, with three on the front side and the other two on the back side. Each TENG unit is made by an aluminum foil as the electrode and a 12.5  $\mu\text{m}$  thick FEP film bonded by another aluminum foil as the dielectric layer. The scanning electron microscope (SEM) image of the FEP film surface is shown in **Figure S1** in the Supporting Information. In the structure of each TENG unit, the introduction of flexible foam is to improve the contact intimacy between triboelectric materials. Further details of fabrication process can be found in the Experimental Section.

**Figure 1b** shows a photograph of as-fabricated spherical TENG device, and the inset shows the photograph of the device in the water waves. The working principle of each TENG unit is demonstrated in **Figure 1c**. First, under the pressing of mass block, the top aluminum foil and the FEP film get contacts and create positive triboelectric charges on the top electrode and negative ones on the FEP surface (state i). Then the separation between the top electrode and FEP film produces an electric potential difference between the two electrodes, which drives free electrons to flow from the bottom electrode to the top one (state ii). The current is generated until they arrive at the maximum separation (state iii). When the two surfaces

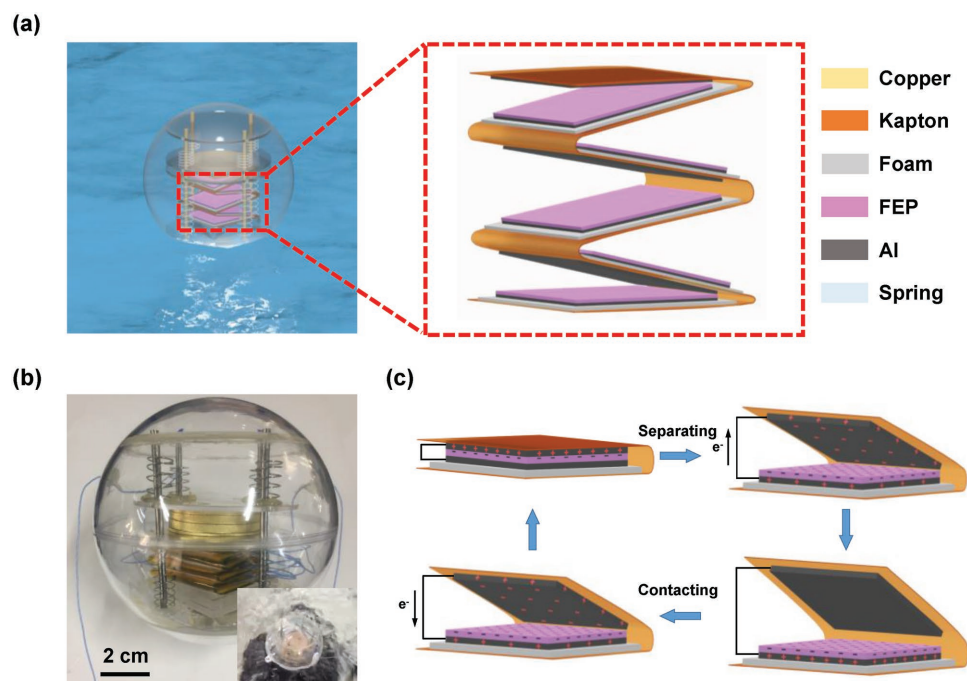


**Figure 1.** a) Schematic diagram of the spherical TENG with spring-assisted multilayered structure floating on water, and schematic representation enlarged structure for the zigzag multilayered TENG with five basic units. b) Photographs of the as-fabricated TENG device. c) Working principle of each TENG unit of the spherical TENG.

of top electrode and FEP film get close to each other again until complete contact, free electrons flow back from the top electrode to the bottom one, generating reversed current flow (state iv). The periodic movement of the mass block under the triggering of water waves, which leads to the contact and separation between two surfaces of the top aluminum foil and FEP film, produces periodic electric output signals.

A spherical TENG device with a spring-assisted and zigzag multilayered structure by integrating five TENG units in parallel was fabricated. After sealing and waterproofing process, the spherical device was placed into the water tank. A function generator was applied to drive a series of wave pumps in the water tank to generate water waves. The frequency and amplitude of water waves were controlled by the output frequency and output amplitude of the signal source. Note that the wave amplitude (wave height) is difficult to be measured directly for the instability of water waves, but because it is approximately proportional to the output voltage amplitude of the function generator ( $H_{out}$ ), the amplitude  $H_{out}$  was adopted as a variable to reflect amplitude of water waves in this work. When triggered by water waves, the outside shell and the mass block both rise, but owing to the existence of the springs, there is a phase difference between these two motions, leading to a relative motion of the mass block and contact-separation movement of each TENG.

The typical electrical output performance of the spherical TENG unit under the water wave motions is presented in Figure 2a–d. The wave frequency was set as 1.0 Hz, and the amplitude  $H_{out}$  and the mass  $m$  of copper block were fixed at 2.5 V and 100 g, respectively. Under the employed experimental conditions, the output current, transferred charges, and output

voltage reached 80  $\mu$ A, 0.52  $\mu$ C, and 420 V, respectively. Note that the peaks of current, charges, and voltage are not uniform, because of the random motion of the water waves. In our work, the TENGs work in a vertical contact-separation mode. According to the theory of contact-separation mode TENG,<sup>[34]</sup> the open-circuit voltage is always positive, ranging from zero to the maximum value. Although we cannot capture the real open-circuit voltage by the Keithley 6514 System Electrometer with capacitive impedance, the influence of the electrometer impedance is not great to ensure the measuring accuracy. So, the measured output voltage signals are always positive. Regarding the issue that the baseline seems not to be at zero, the TENG units may not be fully compressed into the complete contact state by the mass block when triggered by the water waves. Figure 2d shows the average current peak and average power peak as functions of the resistance. It can be found that the TENG device with five units could produce a maximum peak power of 6.79 mW at the matched resistance of 4.7 M $\Omega$ . Note that through the time integral of instantaneous output power in one cycle, the average power of one spherical unit was established to range from one-tenth to one-third of the peak power.<sup>[32,33]</sup>

We are emphasizing that the humidity around the TENG device can have great influences on the output performance of TENG. The outputs of TENG decrease markedly with the increasing of humidity, which has already been indicated in previous works.<sup>[35–37]</sup> Similarly, in our work, the increasing of humidity caused by moisture infiltration will decrease the performance of TENG device. Therefore, the spherical TENG devices have to be well sealed and waterproofed, and the material quality of spherical shell should be appropriate as well as the

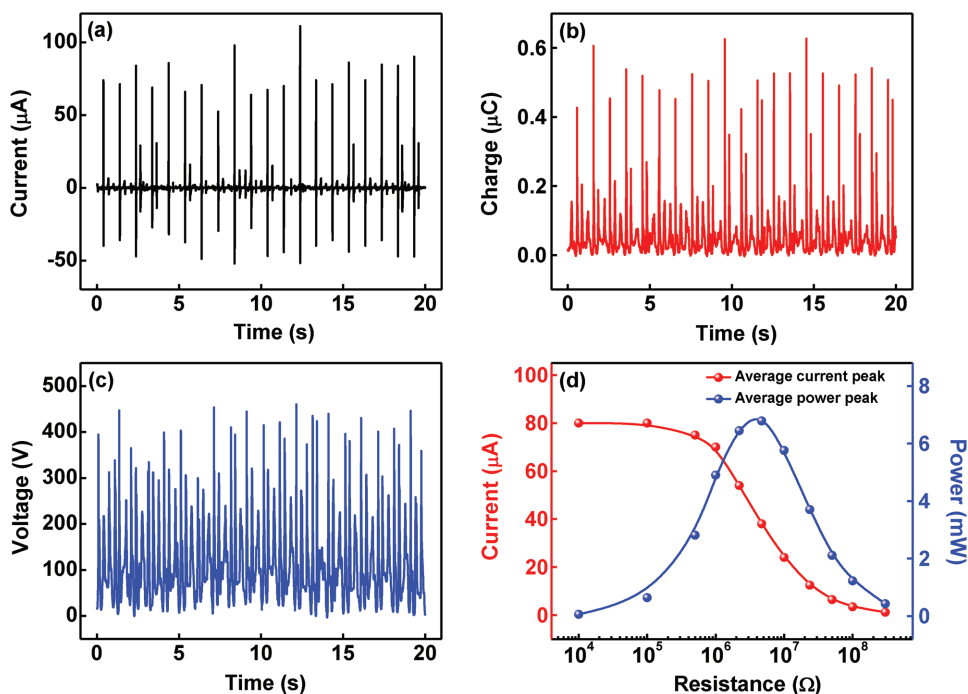


**Figure 2.** a) Typical output current, b) transferred charges, and c) output voltage of the spherical TENG with five units under the water waves. d) Average current peak and average power peak-resistance relationships of the spherical TENG device with five units under the water waves. The water wave frequency, the copper block mass, and the output amplitude of function generator are 1.0 Hz, 100 g, and 2.5 V, respectively.

shell thickness. Our TENGs with well sealed by the tile cement can have only slight decreases in the electric outputs after 4 months from the first measurements, implying that there is little moisture infiltration or humidity change (but the inside humidity is difficult to measure because of the device sealing).

Subsequently, we investigated the influences of the water wave frequency on the output performance of the spherical TENG. The output current, transferred charges, and output voltage for the TENG device as functions of the wave frequency are shown in Figure 3a–c. The amplitude  $H_{out}$  and mass  $m$  of copper block were fixed at 2.5 V and 100 g. As the frequency of the water waves increases from 0.5 to 2.0 Hz, the peak values of output current, transferred charges, and output voltage all first increase and then decrease, exhibiting the maximum values at the frequency of 1.0 Hz. The drop of performance above 1.0 Hz is because that at higher frequencies, the rising mass block at one triggering cannot fall to press the TENG part sufficiently due to another quick triggering. This phenomenon can also be demonstrated in Figure S2a–c in the Supporting Information, showing the output current, transferred charges, and output voltage of the TENG device at  $m = 75$  g under the same experimental conditions. The results indicate that the highest values of 72  $\mu$ A, 353 nC, and 210 V are all obtained at 1.0 Hz. Figure 3d illustrates the output power of the spherical TENG for different frequencies. It can be clearly found that the output power at 1.0 Hz is the highest, reaching 6.79 mW at the matched resistance of 4.7 M $\Omega$ , having a similar tendency to the current, charges, and voltage. However, the matched resistance decreases from 10 to 2.21 M $\Omega$  with increasing the wave frequency.

Besides the water wave frequency, the influence of the wave amplitude reflected by the output voltage amplitude of the function generator ( $H_{out}$ ) was also studied. The output characteristics of the spherical TENG device with five basic units were measured under different  $H_{out}$ , as shown in Figure 4a–d. As can be seen from Figure 4a–c, the output current, transferred charges, and output voltage all increase with increasing the  $H_{out}$ , which implies that a larger wave amplitude is beneficial to produce a higher performance of TENG device. When the value of  $H_{out}$  increases from 1.2 to 2.5 V, the current, charges, and voltage are respectively enhanced by 515.4%, 161.8%, and 50.3%. The output power–resistance relationships of the TENG at various  $H_{out}$  are displayed in Figure 4d. The output power was found to increase with the increase of the  $H_{out}$ . The maximum output power at  $H_{out} = 2.5$  V reaches 6.79 mW, with an enhancement of 1840% compared with the power at  $H_{out} = 1.2$  V (only 0.35 mW). Note that the lower output performance at lower  $H_{out}$  is ascribed to its own weight of the TENG device which cannot be driven by the slight water waves.

In the single spherical TENG device, the mass of copper block and the basic unit number of the zigzag multilayered TENG are two important structural parameters governing the output performance of the device, as well as the external water wave conditions. The internal structure of the spherical TENG device was optimized to generate higher outputs. The output current, transferred charges, and output voltage of the TENG devices fabricated with different  $m$  were measured as shown in Figure 5a,b and Figure S3a in the Supporting Information. The masses  $m$  of 50, 75, and 100 g were chosen for example, while the  $H_{out}$  and the water wave frequency were fixed at 2.5 V and

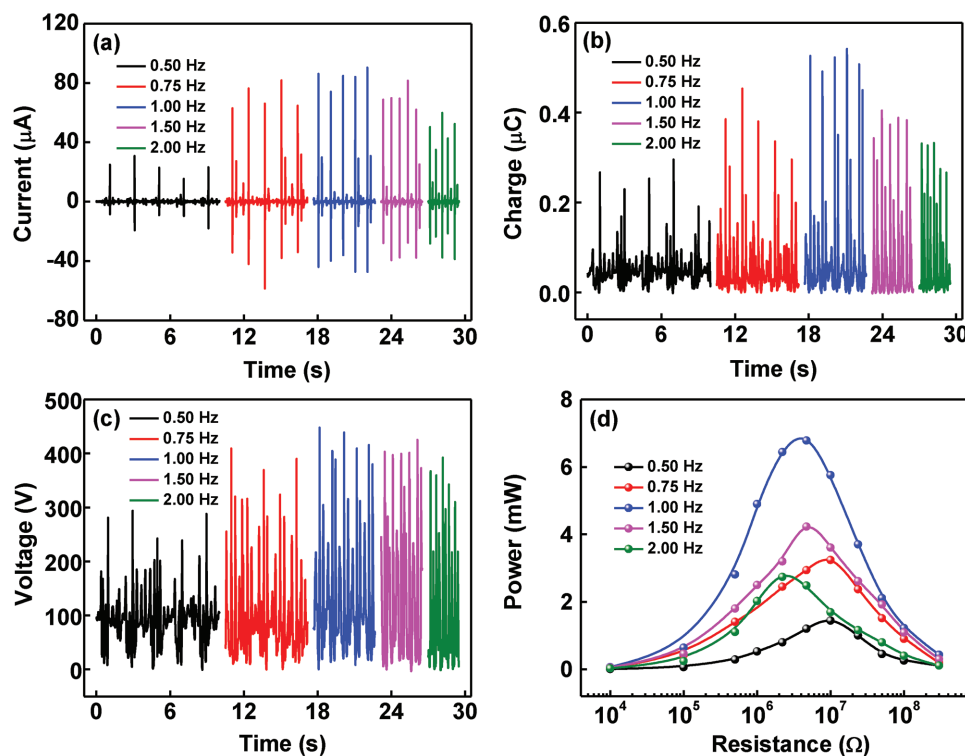


**Figure 3.** a) Output current, b) transferred charges, c) output voltage, and d) output power–resistance profiles of the spherical TENG with five units at various frequencies of water waves. The copper block mass and the output amplitude of function generator are fixed at 100 g and 2.5 V, respectively.

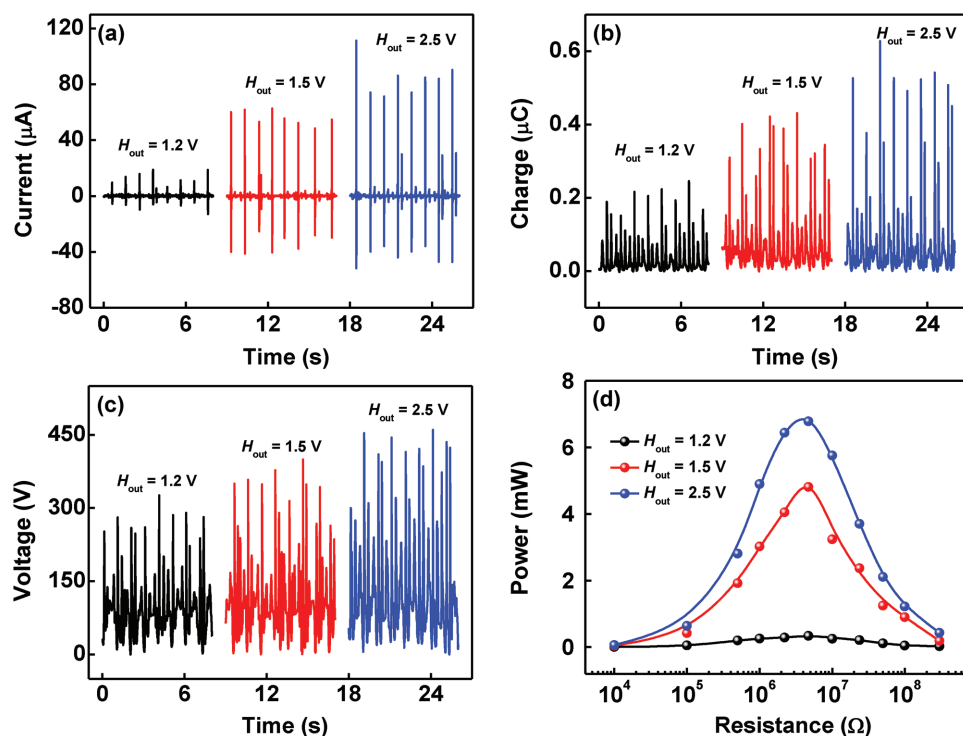


**Figure 4.** a) Output current, b) transferred charges, c) output voltage, and d) output power-resistance relationships of the spherical TENG based on the spring-assisted multilayered structure with five units at different output amplitudes of function generator. The water wave frequency and the copper block mass are fixed at 1.0 Hz, and 100 g, respectively.

1.0 Hz. With increasing  $m$  from 50 to 100 g, the peak values of current, charges, and voltage all increase, because the heavier mass brings more sufficient material surface contact for each TENG unit. As shown in Figure 5c, the output power of the TENG device increases from 1 to 6.79 mW, which is enhanced by 579%. Although increasing the mass of the copper block can enhance the outputs of TENG, too heavy mass block is inadvisable, because that will require a large enough amplitude of water waves and easily damage the TENG device. For a given wave amplitude, the TENG units will be difficult to move under the pressing of so heavy mass block, resulting in lower outputs. So, there is an optimal copper mass for the TENG device to reach the highest outputs.

On the other hand, the effect of basic unit number in the multilayered structure was addressed. The output characteristics of the TENG devices with three, five, and seven basic units are illustrated in Figure 5d–f and Figure S3b in the Supporting Information. With increasing the unit number, the output current, transferred charges, output voltage, and output power all increase, and the spherical device with seven units has the highest values of 120  $\mu\text{A}$ , 0.67  $\mu\text{C}$ , 560 V, and 7.96 mW. The peak power at the matched resistance of 2.21 M $\Omega$  corresponds to a power density of 15.20  $\text{W m}^{-3}$ , according to the volume of the spherical shell. The decrease in the matched resistance of the TENG with seven units compared with the TENG with five units is attributed to the increase of total capacitance, according to the matched resistance expression of  $1/\omega C$ .<sup>[10]</sup> The total capacitance of TENG with seven units, which can be considered as the parallel capacitance of seven sub-capacitors, is larger than that of TENG with five units. The typical output profiles of

the TENG with seven units are also shown in Figure S4a–d in the Supporting Information, where the  $H_{\text{out}}$  and  $m$  are fixed at 2.5 V and 100 g. Regarding the effect of unit number, if the unit number further increases, the motion space of units will be restricted, and also the pressing of the mass block on the units becomes difficult due to the increased elastic force from the units. These will cause the TENG outputs to drop, so there is also an optimal unit number. The effect of the unit number will be examined carefully in our future study.

Here, we had also studied the frequency-dependent output behaviors of the spherical TENG at different wave amplitudes and different basic unit numbers. We found that the TENG devices all exhibit the maximum outputs at the water wave frequency of about 1.0 Hz. The wave amplitude and basic unit number were found to have weak influences on the optimum frequency, as well as the copper block mass. Maybe the optimum frequency is mainly determined by the entire spring-assisted structure of the TENG device with double-spring coupling, rather than the external wave conditions or internal structural details.

Finally, a TENG array consisting of four spherical TENGs with seven basic units was fabricated and measured under the water wave motions. The four spherical units were linked by rigid strings and connected electrically in parallel through four rectifier bridges. A photo of the TENG array device floating on water in a water tank is shown in Figure 6a, where dozens of light-emitting diodes (LEDs) with a “TENG” pattern are lightened up by the array device under the water wave motions (Video S1, Supporting Information). Then the rectified output characteristics were measured at different frequencies of water

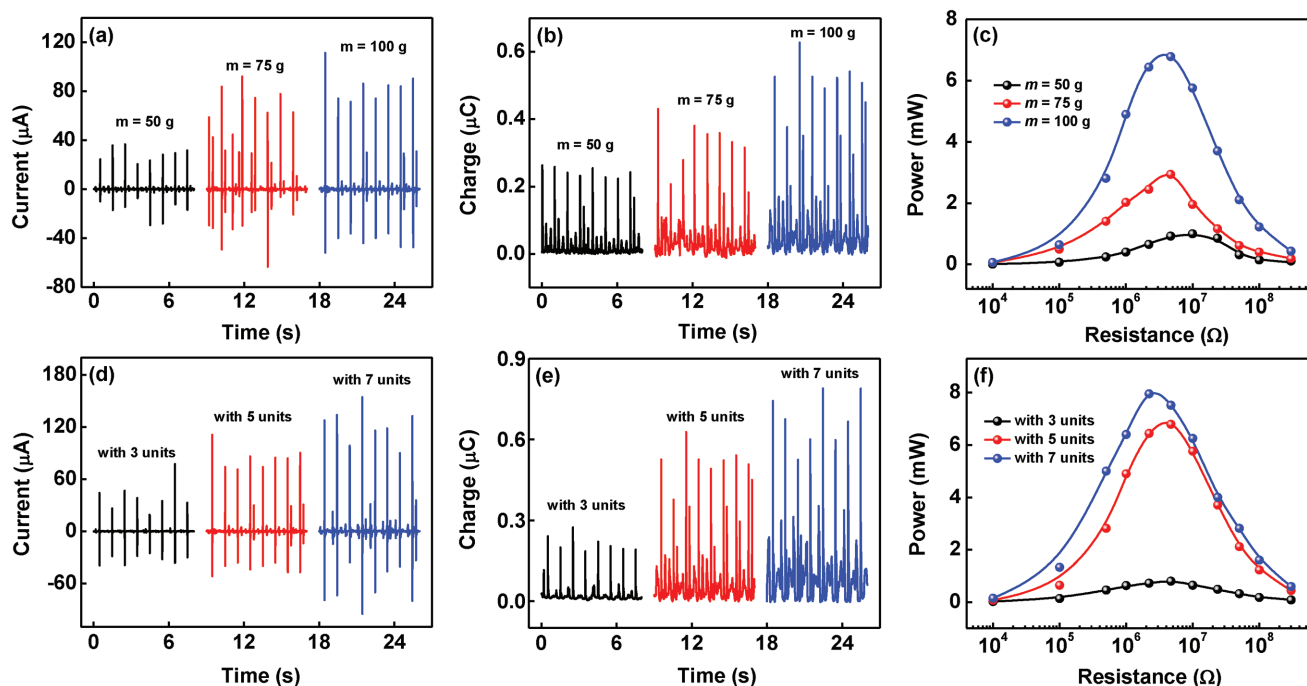


**Figure 5.** Influences of the copper block mass on the a) output current, b) transferred charges, and c) output power-resistance profiles of the spherical TENG with five units. d) Output current, e) transferred charges, and f) output power-resistance profiles for various basic unit numbers in the multi-layered structure at the copper block mass of 100 g. The water wave frequency and the output amplitude of function generator are fixed at 1.0 Hz, and 2.5 V, respectively.

waves from 0.5 to 2.0 Hz, and the  $H_{\text{out}}$  and  $m$  were fixed at 2.5 V and 100 g. As shown in Figure 6b and Figure S5a in the Supporting Information, the outputs of the TENG array first increase with the increasing frequency and then decrease, reaching the maximum values of 225  $\mu\text{A}$  of rectified output current and 340 V of rectified output voltage at 1.0 Hz. In the TENG array, due to different motion states of the four spherical TENGs driven by the water waves, the motion phase sameness is difficult to be fully realized. As a result, the rectified output current of TENG array consisting of four TENG units is not four times than that of single spherical TENG. The decrease of rectified output voltage compared with single spherical TENG is because that the rectified output voltage was measured by the digital oscilloscope. The rectified voltage of the array device cannot be measured by the Keithley 6514 system with capacitive impedance, because the internal capacitor of the electrometer is charged gradually. Instead, we used the digital oscilloscope with resistive impedance. The different measurement principles cause the different values of output voltage. The typical rectified output voltage and current for the TENG array driven by the water waves of 1.0 Hz are presented in Figures S5b and S6 in the Supporting Information. Figure 6c shows the maximum rectified output power of 15.97 mW can be delivered at the matched resistance of 2.21 M $\Omega$  for 1.0 Hz. The matched resistance of the array is roughly the same as one spherical unit, because of the asynchronous movement of different spherical units under the water waves.

The charging and discharging performance of the TENG array was characterized as shown in Figure 6d–f. In Figure 6d, the TENG array at the same wave conditions is used to charge

a capacitor of 470  $\mu\text{F}$ . After the voltage rises to about 1.6 V, an electronic thermometer is connected to the circuit and starts to measure the temperature of the water. The photograph, the charging and discharging process for a capacitor of 470  $\mu\text{F}$  to power the thermometer, and the movie of this process are shown in Figure 6d,e and Video S2 in the Supporting Information, respectively. It can be found from Figure 6e, the charging time of a capacitor of 470  $\mu\text{F}$  by the TENG array is about 159 s. Then the capabilities of the TENG array for charging different capacitors were also investigated, as presented in Figure 6f. The voltage of the capacitor of 1 mF can be raised to 0.74 V within 120 s by the TENG array under the water waves.

### 3. Conclusion

In summary, we designed and fabricated a spherical TENG based on spring-assisted multilayered structure for harvesting water wave energy. The TENG works relying on the contact and separation between the Al electrode and FEP film under the triggering of water waves. The influences of the water wave frequency and amplitude, controlled by the function generator, on the output performance of single spherical TENG device were investigated. And the performance could be further optimized by adjusting the mass of copper block and basic unit number in the multilayered structure. The highest outputs of the TENG with seven basic units were obtained at 1.0 Hz and 2.5 V ( $H_{\text{out}}$ ), reaching 120  $\mu\text{A}$ , 0.67  $\mu\text{C}$ , 560 V, and 7.96 mW, with the corresponding power density of 15.20  $\text{W m}^{-3}$ . Finally, the TENG array consisting of four optimized spherical units connected

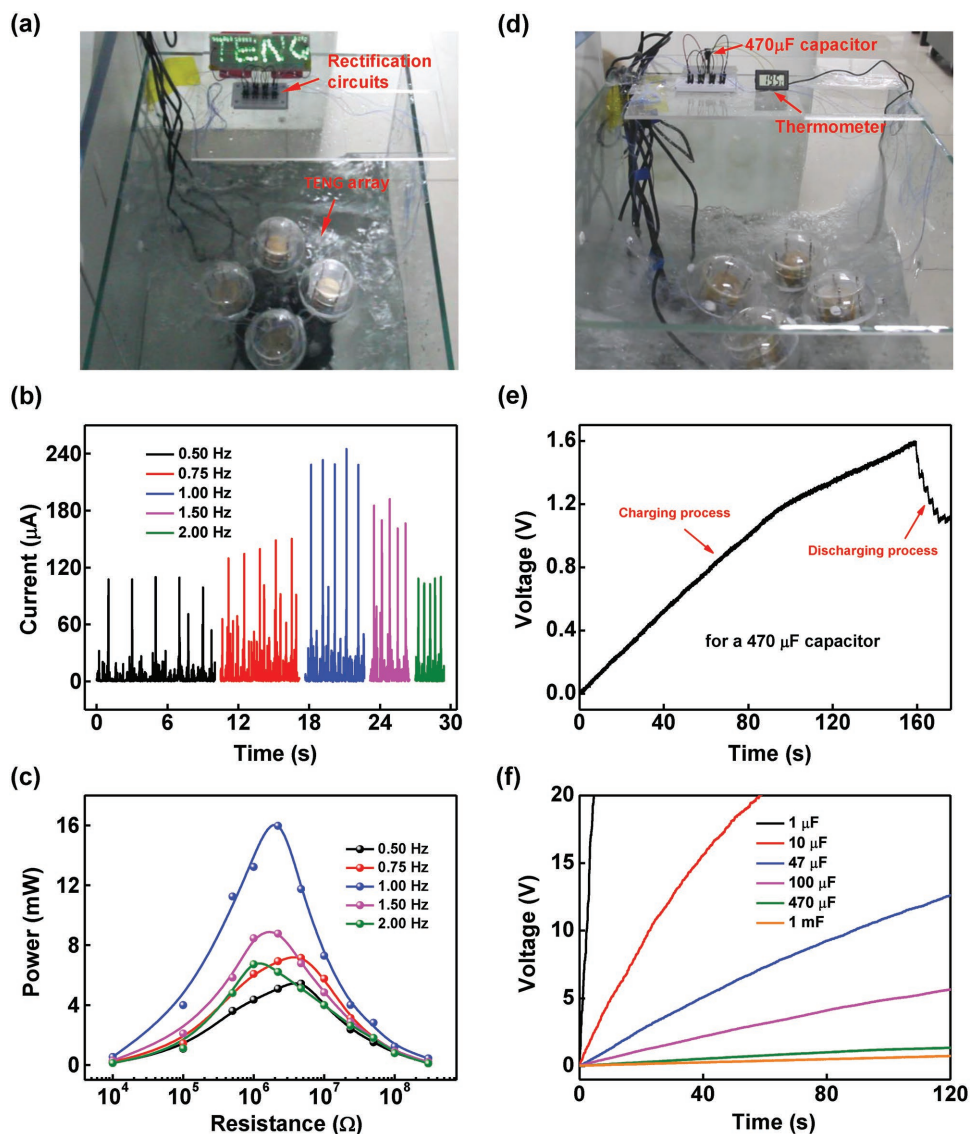


**Figure 6.** a) Photograph of dozens of LEDs with a “TENG” pattern which are lighted up by the TENG array under the water wave motions. b) Rectified output current and c) output power-resistance profiles of the TENG array at various frequencies of water waves. d) Photograph of an electronic thermometer driven by the TENG array under the water wave motions through charging a capacitor of 470  $\mu\text{F}$ . e) The charging and discharging process of a capacitor of 470  $\mu\text{F}$  by the TENG array under the water waves. f) The voltage of various capacitors charging by the TENG array.

in parallel was fabricated, producing 15.97 mW at the matched resistance of 2.21 M $\Omega$ . And dozens of LEDs were lighted up and an electronic thermometer was successfully powered by the TENG array, demonstrating the potential application in large-scale blue energy harvesting.

#### 4. Experimental Section

**Fabrication of the Spherical TENG Device:** First, a 50  $\mu\text{m}$  thick Kapton film with evenly spaced intervals of 4 cm was used as the substrate for TENG units on both sides. In each TENG unit, an aluminum foil with a dimension of 3 cm  $\times$  3 cm was attached on one interval of the Kapton as an electrode, while a 12.5  $\mu\text{m}$  thick FEP film (3 cm  $\times$  3 cm) attached on another aluminum foil as dielectric layer was bonded with a flexible foam to enhance the output performance. The FEP-Al film and foam

as a whole were attached on the adjacent interval of the Kapton. After that, each TENG unit was polarized and connected in parallel, and then the Kapton was shaped to a zigzag structure by making deformations at evenly spaced intervals. Second, two 2 mm thick circular acrylic blocks with four holes were adhered to two semispheres with an outside diameter of 10 cm. On the bottom of the circular acrylic block, four flexible springs with a length of 4.5 cm and four steel shafts with a length of 7.5 cm were attached to sustain the mass block. The mass block consisted of two 2 mm thick circular acrylic blocks and a copper block ( $m$ ) sandwiched in between. Third, four rigid springs with a length of 1.5 cm were adhered to the top side of the mass block. At last, the multilayered TENG with two 4 cm thick acrylic blocks bonded on the bottom side was adhered on the bottom circular acrylic block. After that, the spherical TENG device based on spring-assisted multilayered structure was obtained. In the device, we chose the tribosurface area of 3 cm  $\times$  3 cm, because there is no enough space for larger multilayered TENG due to the unique spherical structure and occupied space of spring, steel shafts, and other related structures.

For the water wave energy harvesting, the sealing and waterproofing were processed on the TENG by using the tile cement. The part A and part B of tile cement were first mixed in the volume ratio of 1:1. Then the mixture was stirred until well distributed. At last, the mixture was applied to the edge of two semispherical acrylic shells for sealing. Regarding the conducting wire connection, in each spherical TENG, the conducting wires in multilayered structure were connected in parallel first, and then were in connection with the rectifiers through the holes of upper semispherical acrylic shell. Four TENGs were respectively connected to a full-bridge rectifier and then connected in parallel.

*Electric Measurements of the TENG Device:* The basic electric outputs of single TENG device and TENG array device were measured under the water waves generated by using a series of wave pumps (rw-20 JEPower TECHNOLOGY Inc.) controlled by a function generator (AFG3011C Tektronix Inc.). The output current, transferred charges, and output voltage of the TENG were measured by a current preamplifier (Keithley 6514 System Electrometer), but in particular the rectified output voltage of the TENG array was measured by a digital oscilloscope (Agilent InfiniiVision 2000X).

## Supporting Information

Supporting Information is available from the Wiley Online Library or from the author.

## Acknowledgements

T.X., X.L., and T.J. contributed equally to this work. Support from the National Key R & D Project from Minister of Science and Technology (2016YFA0202704), the Beijing Municipal Science & Technology Commission (Z17110000317001), National Natural Science Foundation of China (Grant No. 51432005, 51702018, and 51561145021). Project funded by China Postdoctoral Science Foundation (2016M590070), and the “thousands talents” program for the pioneer researcher and his innovation team are appreciated.

## Conflict of Interest

The authors declare no conflict of interest.

## Keywords

blue energy harvesting, multilayered structures, spherical triboelectric nanogenerators, spring-assisted, water wave energy

Received: April 17, 2018

Revised: May 30, 2018

Published online:

- 
- [1] J. P. Painuly, *Renewable Energy* **2001**, *24*, 73.  
 [2] A. Khaligh, O. Onar, *Energy Harvesting: Solar, Wind, and Ocean Energy Conversion Systems*, CRC Press, Boca Raton, FL, USA **2009**.  
 [3] Z. L. Wang, J. Chen, L. Lin, *Energy Environ. Sci.* **2015**, *8*, 2250.  
 [4] Z. L. Wang, *Nature* **2017**, *542*, 159.

- [5] S. H. Salter, *Nature* **1974**, *249*, 720.  
 [6] S. P. Beeby, R. N. Torah, M. J. Tudor, P. Glynne-Jones, T. O. Donnell, C. R. Saha, S. Roy, *J. Micromech. Microeng.* **2007**, *17*, 1257.  
 [7] A. Wolfbrandt, *IEEE Trans. Magn.* **2006**, *42*, 1812.  
 [8] A. Von Jouanne, *Mech. Eng.* **2006**, *128*, 24.  
 [9] F.-R. Fan, Z.-Q. Tian, Z. L. Wang, *Nano Energy* **2012**, *1*, 328.  
 [10] T. Jiang, X. Chen, C. B. Han, W. Tang, Z. L. Wang, *Adv. Funct. Mater.* **2015**, *25*, 2928.  
 [11] Y. Yao, T. Jiang, L. Zhang, X. Chen, Z. Gao, Z. L. Wang, *ACS Appl. Mater. Interfaces* **2016**, *8*, 21398.  
 [12] Z. L. Wang, T. Jiang, L. Xu, *Nano Energy* **2017**, *39*, 9.  
 [13] J. Nie, Z. Ren, J. Shao, C. Deng, L. Xu, X. Chen, M. Li, Z. L. Wang, *ACS Nano* **2018**, *12*, 1491.  
 [14] Y. Bai, C. B. Han, C. He, G. Q. Gu, J. H. Nie, J. J. Shao, T. X. Xiao, C. R. Deng, Z. L. Wang, *Adv. Funct. Mater.* **2018**, *28*, 1706680.  
 [15] X. Cao, M. Zhang, J. Huang, T. Jiang, J. Zou, N. Wang, Z. L. Wang, *Adv. Mater.* **2018**, *30*, 1704077.  
 [16] D. H. Kim, H. J. Shin, H. Lee, C. K. Jeong, H. Park, G. T. Hwang, H. Y. Lee, D. J. Joe, J. H. Han, S. H. Lee, J. Kim, B. Joung, K. J. Lee, *Adv. Funct. Mater.* **2017**, *27*, 1700341.  
 [17] H. S. Wang, C. K. Jeong, M. H. Seo, D. J. Joe, J. H. Han, J. B. Yoon, K. J. Lee, *Nano Energy* **2017**, *35*, 415.  
 [18] Z. L. Wang, *Mater. Today* **2017**, *20*, 74.  
 [19] T. Jiang, Y. Yao, L. Xu, L. Zhang, T. Xiao, Z. L. Wang, *Nano Energy* **2017**, *31*, 560.  
 [20] Z. C. Quan, C. B. Han, T. Jiang, Z. L. Wang, *Adv. Energy Mater.* **2016**, *6*, 1501799.  
 [21] J. Wang, S. M. Li, F. Yi, Y. L. Zi, J. Lin, X. F. Wang, Y. L. Xu, Z. L. Wang, *Nat. Commun.* **2016**, *7*, 8.  
 [22] L. Xu, Y. Pang, C. Zhang, T. Jiang, X. Chen, J. Luo, W. Tang, X. Cao, Z. L. Wang, *Nano Energy* **2017**, *31*, 351.  
 [23] Y. Yang, H. Zhang, R. Liu, X. Wen, T. C. Hou, Z. L. Wang, *Adv. Energy Mater.* **2013**, *3*, 1563.  
 [24] X. F. Wang, S. M. Niu, Y. J. Yin, F. Yi, Z. You, Z. L. Wang, *Adv. Energy Mater.* **2015**, *5*, 1501467.  
 [25] S. H. Wang, L. Lin, Z. L. Wang, *Nano Energy* **2015**, *11*, 436.  
 [26] Q. Jiang, B. Chen, K. W. Zhang, Y. Yang, *ACS Appl. Mater. Interfaces* **2017**, *9*, 43716.  
 [27] B. Dudem, N. D. Huynh, W. Kim, D. H. Kim, H. J. Hwang, D. Choi, J. S. Yu, *Nano Energy* **2017**, *42*, 269.  
 [28] P. Bai, G. Zhu, Z. H. Lin, Q. Jing, J. Chen, G. Zhang, J. Ma, Z. L. Wang, *ACS Nano* **2013**, *7*, 3713.  
 [29] Y. Bian, T. Jiang, T. Xiao, W. Gong, X. Cao, Z. Wang, Z. L. Wang, *Adv. Mater. Technol.* **2018**, *3*, 1700317.  
 [30] T. X. Xiao, T. Jiang, J. X. Zhu, X. Liang, L. Xu, J. J. Shao, C. L. Zhang, J. Wang, Z. L. Wang, *ACS Appl. Mater. Interfaces* **2018**, *10*, 3616.  
 [31] T. Jiang, L. M. Zhang, X. Y. Chen, C. B. Han, W. Tang, C. Zhang, L. Xu, Z. L. Wang, *ACS Nano* **2015**, *9*, 12562.  
 [32] L. Xu, T. Jiang, P. Lin, J. J. Shao, C. He, W. Zhong, X. Y. Chen, Z. L. Wang, *ACS Nano* **2018**, *12*, 1849.  
 [33] C. Wu, R. Liu, J. Wang, Y. Zi, L. Lin, Z. L. Wang, *Nano Energy* **2017**, *32*, 287.  
 [34] S. M. Niu, S. H. Wang, L. Lin, Y. Liu, Y. S. Zhou, Y. F. Hu, Z. L. Wang, *Energy Environ. Sci.* **2013**, *6*, 3576.  
 [35] H. Y. Guo, J. Chen, L. Tian, Q. Leng, Y. Xi, C. G. Hu, *ACS Appl. Mater. Interfaces* **2014**, *6*, 17184.  
 [36] D. Kim, S. J. Park, S. B. Jeon, M. L. Seol, Y. K. Choi, *Adv. Electron. Mater.* **2016**, *2*, 1500331.  
 [37] M. L. Seol, J. H. Woo, D. I. Lee, H. Im, J. Hur, Y. K. Choi, *Small* **2014**, *10*, 3887.